

•Research article•

New antibacterial depsidones from an ant-derived fungus *Spiromastix* sp. MY-1

GUO Zhi-Kai^{1,2A}, ZHU Wen-Yong^{1,3A}, ZHAO Li-Xing^{1,4}, CHEN Yan-Chi¹, LI Sui-Jun¹,
CHENG Ping¹, GE Hui-Ming¹, TAN Ren-Xiang¹, JIAO Rui-Hua^{1*}

¹State Key Laboratory of Pharmaceutical Biotechnology, Institute of Functional Biomolecules, School of Life Sciences, Nanjing University, Nanjing 210093, China;

²Hainan Key Laboratory of Tropical Microbe Resources, Institute of Tropical Bioscience and Biotechnology, Chinese Academy of Tropical Agricultural Sciences, Haikou 571101, China;

³Yunnan Key Laboratory of Vaccine Research & Development on Severe Infectious Diseases, Institute of Medical Biology, Chinese Academy of Medical Sciences, Kunming 650118, China;

⁴Yunnan Institute of Microbiology, Yunnan University, Kunming 650091, China

Available online 20 Aug., 2022

[ABSTRACT] Six new (1–6) and seven known depsidones (7–13) were isolated from the culture of an ant (*Monomorium chinensis*)-derived fungus *Spiromastix* sp. MY-1. Their structures were elucidated by extensive spectroscopic analysis including high resolution MS, 1D and 2D NMR data. The new bromide depsidones were obtained through supplementing potassium bromide in the fermentation medium of *Spiromastix* sp. MY-1. All isolated compounds showed various bioactivities against the tested phytopathogenic bacteria. Particularly, new bromide compound 4, named spiromastixone S, exhibited the strongest activity against *Xanthomonas oryzae* pv. *oryzae* with a MIC value of 5.2 $\mu\text{mol}\cdot\text{L}^{-1}$.

[KEY WORDS] Fungus; *Spiromastix* sp.; Depsidones; Phytopathogenic bacteria; Antibacterial

[CLC Number] R284, R965 **[Document code]** A **[Article ID]** 2095-6975(2022)08-0627-06

Introduction

Bacterial blight, caused by *Xanthomonas oryzae* pv. *oryzae* (Xoo), is a devastating rice disease worldwide [1], resulting in annual yield losses up to 60%. It is also one of the most destructive rice diseases in Asia [2, 3]. Therefore, it spurs a social need for highly active agricultural agents in the field of farmland management. Mutualistic microbes with ants are commonly considered as an efficient defense against herbivores [4] as well as plant pathogens [5]. Some species of plant-

mutualistic ants kill the vegetation growing in the vicinities of their host plant to create an area of bare ground [6]. Furthermore, *Macaranga myrmecophyte* plants was infected with fungi without the presence of *Crematogaster* mutualistic ants [7] and fungi-ant-plants symbiosis was considered to be a multipartite symbiotic community [8]. Endophyte-mediated defense is effective against pathogens and non-herbivory damage [9], which suggests the potential role of ant-derived fungi in producing promising natural products against plant pathogens. Therefore, during our ongoing search for new bioactive secondary metabolites from symbiotic fungi inhabiting in ants [10, 11], one strain, *Spiromastix* sp. MY-1, isolated from an ant (*Monomorium chinensis*) collected from the rice field, was shown to be a prolific producer of chlorinated compounds on the basis of ¹H NMR and LC-MS analyses of the extracts derived from cultures of our microbe collection. As bromination and chlorination in the natural product biosynthesis usually share a common biosynthetic pathway [12], we fermented the fungus using Martin fermentation media supplemented with potassium bromide to expand the structural diversity. As a result, six new bromide depsidones, named spiromastixones P–U (1–6) (Fig. 1), together with spiromas-

[Received on] 25-Feb.-2022

[Research funding] This work was supported by the National Key Research and Development Programs (Nos. 2018YFA0902000 and 2017YFC0506200), the National Natural Science Foundation of China (Nos. 81991524 and 81673333), the Hainan Provincial Basic and Applied Basic Research Fund for High-Level Talents in Natural Science (Nos. 2019RC306 and 2019RC352) and the Central Public-interest Scientific Institution Basal Research Fund for CATAS-ITBB (Nos. 1630052019011 and 1630052022016).

[*Corresponding author] E-mail: rhjiao@nju.edu.cn

^AThese authors contributed equally to this work.

These authors have no conflict of interest to declare.

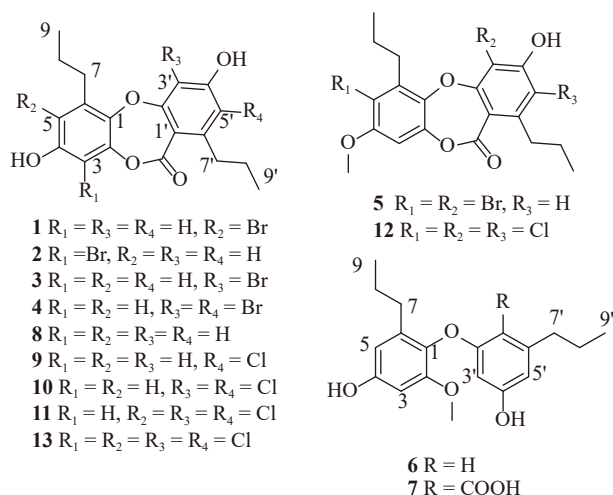


Fig. 1 Structures of the isolated compounds 1–13

tol E (7), spiromastixones A (8), B (9), E (10), F (11), G (12), and I (13) (Fig. 1)^[13,14], were isolated and characterized. Few depsidones have been reported from marine-derived fungi^[15,16] and plant endophytic fungi^[17,18]. This is the first description of depsidone-type natural products from insect-derived fungi. According to previous findings, depsidones exerted a variety of biological activities including antibacterial^[19], antitumor^[20] and herbicidal effects^[21], and HIV integrase inhibition activities^[22]. However, the activity of depsidones against plant pathogens has rarely been reported. In this paper, the antibacterial activity of these isolated depsidones was evaluated using several plant pathogenic bac-

teria. Among the tested compounds, spiromastixone S (4) displayed remarkable activity against *X. oryzae* pv. *oryzae* with an MIC of 5.2 $\mu\text{mol}\cdot\text{L}^{-1}$, which may play a role in protecting ant food and habitat against plant pathogens.

Results and Discussion

The EtOAc extract of the fermentation broth of fungus MY-1 isolated from an ant (*M. chinensis*) was separated by column chromatography followed by semipreparative HPLC purification if necessary, affording compounds 1–13.

The ESI-MS spectrum of spiromastixones P (1) displayed an ions pair $[\text{M} + \text{H}]^+$ at m/z 407 and 409 at a ratio of 1 : 1, indicating the presence of one bromine atom. The molecular formula was established as $\text{C}_{19}\text{H}_{19}^{79}\text{BrO}_5$ on the basis of a pseudomolecular ion peak in the HR-ESI-MS spectrum at m/z 407.0492 (Calcd. for $\text{C}_{19}\text{H}_{20}^{79}\text{BrO}_5^+$, 407.0489), one more bromine atom than that of 8. The ^1H NMR spectrum (Fig. S1) of 1 exhibited three aromatic proton resonances at δ_{H} 6.81 (1H, s, H-3), 6.73 (1H, d, $J = 2.0$ Hz, H-3'), 6.72 (1H, d, $J = 2.0$ Hz, H-5') (Table 1). The ^{13}C NMR (Fig. S2) and HSQC (Fig. S3) spectra showed 12 aromatic carbons, 2 methyls, 4 methylenes and a carbonyl carbon. Based on the ^1H - ^1H COSY (Fig. S4) and HMBC (Fig. S5) correlations (Fig. 2), two *n*-propyl units were directly connected to the C-6 (δ_{C} 136.7) and C-6' (δ_{C} 150.7) according to the HMBC correlations from H₂-7 (δ_{H} 2.99) to C-1 (δ_{C} 143.1), C-5 (δ_{C} 108.7), and C-6 and from H₂-7' (δ_{H} 2.76) to C-1' (δ_{C} 113.1), C-5' (δ_{C} 116.1), and C-6'. Furthermore, the HMBC correlations (Fig. 2) from H-3 (δ_{H} 6.81) to C-1, C-2 (δ_{C} 145.1), C-4

Table 1 ^1H NMR data (500 MHz) for compounds 1–8 (δ_{H} , mult, J in Hz)

No.	1 ^{a,d}	2 ^a	3 ^{a,d}	4 ^b	5 ^a	6 ^c	7 ^c	8 ^{a,d}
3	6.81 s		6.57 d (3.0)	6.49 d (2.5)	6.94 s	6.37 d (2.5)	6.39 d (2.0)	6.48 d (3.2)
5		6.79 s	6.58 d (3.0)	6.48 d (2.5)		6.29 d (2.5)	6.25 d (2.0)	6.49 d (3.2)
7	2.99 (t, 8.0)	2.75 (t, 7.8)	2.98 (t, 9.8)	2.94 (t, 7.8)	3.28 (t, 8.0)	2.29 (t, 7.8)	2.30 (t, 7.5)	2.76 (t, 10.0)
8	1.66 m	1.66 m	1.66 m	1.66 m	1.61 m	1.44 m	1.40 m	1.59 m
9	1.09 t (7.5)	1.01 t (7.5)	1.08 t (7.3)	1.00 t (7.5)	1.07 t (7.5)	0.79 t (7.5)	0.78 t (7.5)	0.93 t (7.2)
1'						6.04 br s		
3'	6.73 d (2.0)	6.72 d (2.0)				5.90 t (2.0)	5.67 d (2.0)	6.54 d (2.4)
5'	6.72 d (2.0)	6.71 d (2.0)	6.90 s		6.93 s	6.16 br s	6.20 d (2.0)	6.55 d (2.4)
7'	2.76 (t, 7.8)	2.79 (t, 7.8)	2.73 (t, 9.8)	2.90 (t, 7.8)	2.74 (t, 7.8)	2.37 (t, 7.5)	2.50 (overlap)	2.80 (t, 9.5)
8'	1.57 m	1.57 m	1.57 m	1.64 m	1.58 m	1.49 m	1.56 m	1.53 m
9'	0.89 t (7.5)	0.88 t (7.5)	0.88 t (7.3)	0.93 t (7.5)	0.89 t (7.5)	0.85 t (7.5)	0.90 t (7.5)	0.87 t (7.2)
2-OMe						3.62 s	3.65 s	
4-OMe					3.92 s			
4-OH						9.25 s	9.32 s	
4'-OH						9.13 s	9.37 s	
1-COOH							12.51 s	

^a Recorded in acetone- d_6 ; ^b Recorded in methonal- d_4 ; ^c Recorded in DMSO- d_6 ; ^d 400 MHz

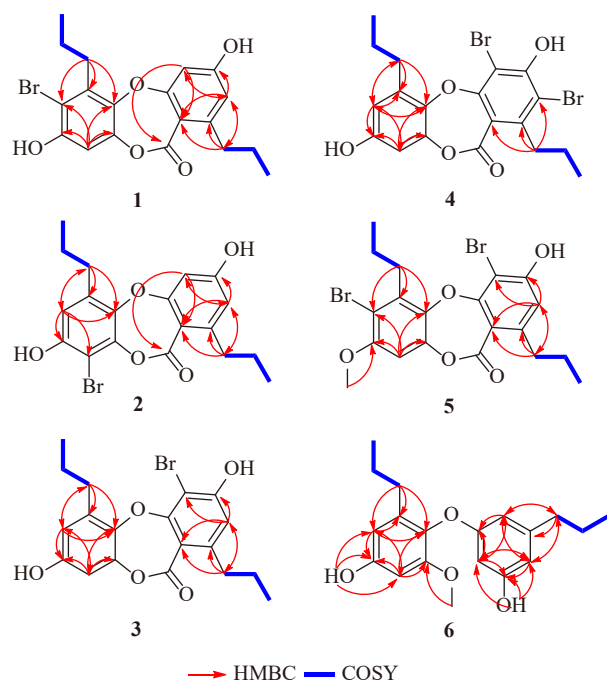


Fig. 2 ^1H - ^1H COSY and HMBC correlations of compounds 1–6

(δ_{C} 152.8) and C-5, from H-3' (δ_{H} 6.73) to C-1', C-5' and the carbonyl carbon at δ_{C} 164.3, and from H-5' (δ_{H} 6.72) to C-1', C-3' (δ_{C} 105.7), C-4' (δ_{C} 163.1) and C-7' (δ_{C} 36.4) indicated the presence of two aromatic rings, one of which was a 1,2,5-trisubstituted 6-propyl-4-hydroxyphenyl ring and the other was a 1',2'-disubstituted 6'-propyl-4'-hydroxyphenyl ring. Compared with the NMR data of the known compound **8** (Tables 1 and 2) (Figs. S51–S55)^[13], the structure of compound **1** was closely similar with **8** with the exception that a methine carbon signal at C-5 (δ_{C} 113.5) for **8** was replaced by a quaternary carbon at δ_{C} 108.7 in **1**. These data indicated that compounds **1** and **8** shared the same skeleton and the hydrogen at C-5 (δ_{C} 113.5) for **8** was substituted by a bromine atom in **1**. This assignment was supported by HMBC correlations (Fig. 2) from H-3 (δ_{H} 6.81) and H₂-7 (δ_{H} 2.99) to C-5.

Spiromastixones Q (**2**) and R (**3**) had the same molecular formula with that of **1** and also displayed similar ^1H and ^{13}C NMR spectra (Tables 1 and 2) to those of **8**. The NMR data (Table 1) (Figs. S8–S19) suggested that bromine atoms in compounds **1**, **2** and **3** were located at different positions. Compared with compound **8**, H-5 (δ_{H} 6.79) showed correlations with C-1 (δ_{C} 143.8), C-3 (δ_{C} 99.8), C-4 (δ_{C} 153.0), C-7 (δ_{C} 33.2) (Fig. 2) for **2** and there was no HSQC correlations for C-3 (δ_{C} 99.8), indicating the C-3 for **2** was brominated.

Table 2 ^{13}C NMR data (125 MHz) for compounds 1–8

No.	1 ^{a,d}	2 ^a	3 ^{a,d}	4 ^b	5 ^a	6 ^c	7 ^c	8 ^{a,d}
1	143.1	143.8	143.3	143.5	144.1	133.0	132.7	142.9
2	145.1	144.1	145.6	145.7	144.9	152.6	152.6	145.9
3	106.2	99.8	106.0	106.0	103.4	98.6	98.5	105.8
4	152.8	153.0	155.9	156.6	155.3	154.7	155.0	155.6
5	108.7	113.3	114.2	114.7	110.7	107.5	107.8	113.5
6	136.7	135.4	137.4	137.7	137.4	136.3	136.4	136.8
7	33.1	32.2	33.8	34.2	33.8	31.4	31.3	32.4
8	23.4	24.2	25.0	25.4	23.7	22.5	22.9	24.5
9	14.4	14.2	14.3	14.2	14.2	13.7	13.6	14.3
1'	113.1	113.1	114.8	116.7	114.0	105.5	115.3	113.0
2'	162.8	162.7	159.4	156.9	159.9	159.7	156.4	163.3
3'	105.7	105.8	99.4	101.1	99.4	98.9	97.8	105.8
4'	163.1	163.1	161.5	160.8	161.4	158.1	158.2	163.7
5'	116.1	116.2	115.5	112.2	115.8	108.3	108.4	116.0
6'	150.7	150.4	149.0	147.2	149.6	144.0	141.2	150.3
7'	36.4	36.3	36.5	37.4	36.6	37.3	35.0	36.5
8'	25.4	25.4	25.3	24.1	25.3	23.7	23.7	25.4
9'	14.3	14.3	14.4	14.2	14.3	13.5	13.9	14.3
1'-C=O	164.3	164.3	163.1	164.1	162.4		169.0	164.5
2-OMe						55.4	55.4	
4-OMe					57.3			

^a Recorded in acetone-*d*₆; ^b Recorded in methanol-*d*₄; ^c Recorded in DMSO-*d*₆; ^d 100 MHz

For compound **3**, H-3 (δ_{H} 6.57) showed HMBC correlations with C-1 (δ_{C} 143.3), C-2 (δ_{C} 145.6), C-4 (δ_{C} 155.9), C-5 (δ_{C} 114.2) and H-5 (δ_{H} 6.58) with C-1, C-3 (δ_{C} 106.0), C-4, C-7 (δ_{C} 33.8), H-5' (δ_{H} 6.90) with C-7' (δ_{C} 36.5), implying that C-3' for **3** was brominated. Thus, the structures of **2** and **3** were determined to be 3- and 3'-brominated **8**, respectively.

Spiromastixones S (**4**) was purified as a white amorphous solid. The HR-ESI-MS spectrum exhibited an isotopic cluster of ions $[\text{M} + \text{Na}]^+$ at m/z 507, 509 and 511 at a ratio of 1 : 2 : 1, indicating the presence of two bromine atoms. The molecular formula of **4** was determined to be $\text{C}_{19}\text{H}_{18}\text{Br}_2\text{O}_5$ by a pseudomolecular ion peak in the HR-ESI-MS spectrum at m/z 506.9413 $[\text{M} + \text{Na}]^+$ (Calcd. for $\text{C}_{19}\text{H}_{18}^{79}\text{Br}_2\text{O}_5\text{Na}^+$, 506.9413), one more bromine atom than **3**. The spectral data (Figs. S22–S26) of compound **4** were very similar to those of spiromastixones R (**3**) (Tables 1 and 2), indicating that both of them shared the same skeleton. However, the H-5' (δ_{H} 6.90) singlet for **3** was missing in **4**, indicating that the hydrogen at C-5' (δ_{C} 115.5) for **3** was substituted by a bromine atom. Thus, the structure was assigned as a 5'-brominated analogue of **3**. This assignment was also supported by the HMBC correlations from H-7' to C-5' (δ_{C} 112.2), C-6' (δ_{C} 147.2) and C-1' (δ_{C} 116.7) (Fig. 2).

Spiromastixones T (**5**), a white amorphous solid, was assigned the molecular formula $\text{C}_{20}\text{H}_{20}\text{Br}_2\text{O}_5$ according to an $[\text{M} + \text{H}]^+$ ion at m/z 498.9749 (Calcd. for $\text{C}_{20}\text{H}_{21}^{79}\text{Br}_2\text{O}_5^+$, 498.9750) with the diagnostic ratio of isotopic ions 1 : 2 : 1 at m/z 499, 501 and 503. The ^1H and ^{13}C NMR data of **5** (Tables 1 and 2) (Figs. S29–S34) showed that it had an identical scaffold with compounds **1–4**. Compared with the ^1H and ^{13}C NMR spectral data of compounds **1**, **3** and **5**, two bromine atoms were assigned to C-5 (δ_{C} 110.7) and C-3' (δ_{C} 99.4) for **5**, respectively, which was also supported by the HMBC interactions (Fig. 2). The HMBC correlation of the methoxy group at δ_{H} 3.92 with C-4 (δ_{C} 155.3) determined that OMe-4 was connected to C-4. Thus, the full structure of **5** was established and named spiromastixones T.

Spiromastixones U (**6**) was obtained as a white amorphous solid. The HR-ESI-MS data deduced its molecular formula as $\text{C}_{19}\text{H}_{24}\text{O}_4$ according to an $[\text{M} + \text{Na}]^+$ ion at m/z 339.1575 (Calcd. for $\text{C}_{19}\text{H}_{24}\text{O}_4\text{Na}^+$, 339.1567). The ^1H and ^{13}C NMR data (Tables 1 and 2) of compound **6** (Figs. S37–S42) were very similar to those of spiromastixones V (**7**)^[14] (Figs. S45–S50) except for an additional proton signal at δ_{H} 6.04 in **6** and the absence of carboxyl carbon signal at δ_{C} 169.0 in **7**, suggesting that **6** is the decarboxylative product of **7**. This assignment was further supported by HMBC correlations (Fig. 2) from H-7' (δ_{H} 2.37) to C-1' (δ_{C} 105.5), C-5' (δ_{C} 108.3) and C-6' (δ_{C} 144.0), and from the exchangeable proton at H-1' (δ_{H} 6.04) to C-2' (δ_{C} 159.7), C-3' (δ_{C} 98.9), C-5', C-6' and C-7' (δ_{C} 37.3). Subsequently, the full structure of **6** was established and named spiromastixones U.

The antibacterial activities of the isolated compounds were tested and the results are listed in Table 3, where kana-

Table 3 Antibacterial activities of compounds **1–13** (MIC value: $\mu\text{mol}\cdot\text{L}^{-1}$)

Compounds	B1	B2	B3	B4	B5
1	6.2	12.3	12.3	12.3	12.3
2	63.2	63.2	63.2	63.2	7.9
3	22.6	11.3	11.3	11.3	11.3
4	5.2	10.4	10.4	10.4	10.4
5	13.8	27.6	27.6	27.6	27.6
6	12.6	12.6	25.2	25.2	6.3
7	-	20.2	-	40.4	20.2
8	5.4	5.4	10.8	10.8	5.4
9	10.1	20.2	-	40.4	-
10	6.2	24.6	24.6	24.6	24.6
11	5.8	11.6	11.6	11.6	23.2
12	21.0	21.0	21.0	21.0	21.0
13	24.6	24.6	24.6	24.6	24.6
kanamycin*	4.3	4.3	0.54	0.54	1.08

Xanthomonas oryzae pv. *oryzae* (B₁), *Xanthomonas oryzae* pv. *oryzicola* (B₂), *Erwinia amylovora* (B₃), *Pseudomonas syringae* pv. *lachrymans* (B₄), *Clavibacter michiganense* subsp. *sepedonicus* (B₅), no activity (-), and kanamycin as the positive control (*).

mycin was used as the positive control. All compounds except **2** and **7** had potent activities against the tested pathogenic bacteria. Especially, compared with the positive control, compounds **4**, **8**, **10** and **11** exhibited significant activities against Xoo, with MIC values of 5.2, 5.4, 6.2 and 5.8 $\mu\text{mol}\cdot\text{L}^{-1}$, respectively. A primary analysis of the structure-activity relationships revealed that the substitution at C-3 resulted in an influence on the inhibition by comparing the activities of compounds **2** and **13** with **8**. The rice bacterial pathogen *X. oryzae* pv. *oryzae* (Xoo) is one of the most severe pathogenic bacteria in rice cultivation^[23]. The antibacterial activity test against Xoo revealed that compound **4** may be a potent bactericide lead for controlling rice bacterial blight disease. These findings suggested that rice plant-ant-fungus may act as a mutualistic system, from which the ant-associated fungi produce antibiotics to help protect their gardens from pathogens. Thus the ant-associated fungi in rice plantation system may be a promising source of bactericide against rice pathogens.

In conclusion, six new depsidone-type natural products, spiromastixones P–U (**1–6**), were identified from the ant-associated fungus *S. sp.* MY-1, representing a new class of depsidone derivatives with unusual brominated substitutions. The most exciting finding is the discovery of a new bromide depsidone, spiromastixones S (**4**) which displays significant inhibitory activity against rice bacterial blight disease Xoo with the similar MIC value as that of kanamycin, indicating its promising potential as a bactericide to control the phytopath-

ogen Xoo. This study also suggests that the insect-associated fungi have the potential to produce bioactive compounds. Furthermore, changing cultural medium may be an effective way to obtain novel bioactive halogenated compounds.

Experimental

General experimental procedures

HR-ESI-MS spectra were recorded on an Agilent 6210 TOF LC-MS instrument (Agilent Technologies Inc., Palo Alto, USA). IR spectra were obtained on a Nexus 870 FT-IR spectrometer (Thermo Nicolet Corporation, Madison, USA). NMR spectra were recorded on a Bruker AV-500/400NMR spectrometer (Bruker Corporation, Karlsruhe, Germany). UV spectra were recorded on a Hitachi U-3000 spectrophotometer (Hitachi, Ltd., Tokyo, Japan). Silica gel (200–300 mesh; Qingdao Marine Chemical Factory, Qingdao, China) and Sephadex LH-20 gel (Pharmacia Biotech, Sweden) were used for column chromatography (CC). HPLC was performed with a Hitachi L-7110 pump and L-7400 UV detector equipped with an Apollo C₁₈ column (5 μm, 250 mm × 4.6 mm; Alltech Associates, Inc. Chicago, IL, USA).

Fungal material

The strain MY-1 was isolated from an ant *M. chinensis* collected in October 2011 from the suburb of Nanjing, Jiangsu Province, China. It was identified by 18S rDNA gene sequence analysis. The 18S rDNA sequence of this strain has been deposited at GenBank under the accession number KC952004. Phylogenetic analysis based on 18S rDNA gene sequences revealed that strain MY-1 belongs to the genus *Spiromastix* (Fig. S82).

Fermentation and fractionation using Martin solution with running water

After growing on PDA medium at 28 °C for 7 days, the fungus *Spiromastix* sp. MY-1 was inoculated into Erlenmeyer flasks (1 L) containing 400 mL of Martin solution (10.0 g of sucrose, 5.0 g of peptone, 0.5 g of yeast extract, 0.5 g of MgSO₄·7H₂O, 1.0 g of K₂HPO₄, and 1.0 L of running water). After incubation at 28 °C on a rotary shaker at 108 r·min⁻¹ for 5 days, 20 mL of culture liquid was transferred to 1000 mL Erlenmeyer flasks containing 400 mL of Martin solution. These flasks were incubated at 28 °C on a rotary shaker at 110 r·min⁻¹ for 21 days. After fermentation, the culture (45 L) was filtered to yield the filtrate and a mycelial cake. The filtrate was extracted with an equal volume of EtOAc for three times. The extracts were combined and the solvent was removed under reduced pressure. The mycelial cake was extracted with 2 L of methanol for three times. The organic layers were combined and the solvent was removed under reduced pressure. Then, the two organic extracts were combined to give 5.26 g of residue. The residue was subjected to silica gel CC using gradient elution with a mixture of CH₂Cl₂ : MeOH (100 : 0, 100 : 1, 100 : 2, 100 : 4, 100 : 8, 100 : 16, and 0 : 100, V/V) to give seven fractions (Fr.1–Fr.7), respectively. Fr.3 was purified by semipreparative HPLC with an ODS column using an elution system consisting of 66%

methanol in water containing 0.1% trifluoroacetic acid (TFA) (2.5 mL·min⁻¹, UV at 254 nm) to give **8** (3.2 mg, t_R 150 min). Purification of Fr.2 by Sephadex LH-20 and semipreparative HPLC (66% methanol with 0.1% TFA) gave **9** (5.2 mg, t_R 69.5 min), **10** (18.0 mg), **11** (7.2 mg, t_R 46.2 min) and **12** (4.3 mg, t_R 80.3 min). Fr.3 was purified by semipreparative HPLC (88% methanol containing 0.1% TFA) to give **13** (23 mg, t_R 20.5 min).

Fermentation and fractionation using Martin solution with deionized water supplemented with potassium bromide

The Martin solution for seed culture and large-scale fermentation was supplemented with 25 mmol·L⁻¹ KBr, using deionized water instead of running water. After fermentation, the culture (45 L) was separated into the supernatant and mycelial cake. The mycelial cake was extracted with 2 L of methanol for three times. The extracts were combined and the organic solvent was removed under reduced pressure to afford 4.8 g of a residue for further purification. This residue was subjected to silica gel CC using gradient elution with a mixture of CH₂Cl₂ : MeOH (100 : 0, 100 : 1, 100 : 2, 100 : 4, 100 : 8, 100 : 16, 0 : 100, V/V) to give seven fractions (Fr.1–Fr.7), respectively. Fr.4 was purified by semipreparative HPLC (73% methanol containing 0.1% TFA) to give **6** (28 mg, t_R 7.8 min) and **7** (5.4 mg, t_R 3.5 min). Purification of Fr.2 by semipreparative HPLC (65% methanol containing 0.1% TFA) gave **1** (6.2 mg, t_R 81.2 min), **2** (5.1 mg, t_R 50.5 min), **3** (4.3 mg, t_R 64.4 min), and **4** (4.7 mg, t_R 143.4 min). Fr.4 was purified by Sephadex LH-20 and gave **5** (3.7 mg).

Spiromastixones P (1): a white amorphous solid; UV (MeOH): λ_{max} (log ε) 230 (3.7), 269 (3.1) nm; IR (KBr) ν_{max}: 3401, 3245, 2964, 2937, 2873, 1704, 1609, 1429, 1216, 1144, 1110, 1004, 850 cm⁻¹; HR-ESI-MS m/z 407.0492 ([M + H]⁺, Calcd. for C₁₉H₂₀BrO₅⁺, 407.0489).

Spiromastixones Q (2): a white amorphous solid; UV (MeOH): λ_{max} (log ε) 225 (3.8), 262 (3.4) nm; IR (KBr) ν_{max}: 3385, 3219, 2963, 2932, 2873, 1681, 1609, 1430, 1205, 1148, 1104 cm⁻¹; HR-ESI-MS m/z 407.0492 ([M + H]⁺, Calcd. for C₁₉H₂₀BrO₅⁺, 407.0489).

Spiromastixones R (3): a white amorphous solid, UV (MeOH): λ_{max} (log ε) 221 (4.0), 269 (3.4), 306 (3.2) nm; IR (KBr) ν_{max}: 3330, 2960, 2927, 2870, 1707, 1592, 1411, 1200, 1142, 1104, 850 cm⁻¹; HR-ESI-MS m/z 407.0487 ([M + H]⁺, Calcd. for C₁₉H₂₀BrO₅⁺, 407.0489).

Spiromastixones S (4): a white amorphous solid; UV (MeOH): λ_{max} (log ε) 222 (3.3), 287 (2.7), 320 (2.8) nm; IR (KBr) ν_{max}: 3354, 2956, 2928, 2870, 1705, 1562, 1460, 1404, 1257, 1141, 1107, 844 cm⁻¹; HR-ESI-MS m/z 506.9413 ([M + Na]⁺, Calcd. for C₁₉H₁₈Br₂O₅Na⁺, 506.9413).

Spiromastixones T (5): a white amorphous solid; UV (MeOH): λ_{max} (log ε) 228 (3.1), 254 (2.6), 289 (2.6), 317 (2.8) nm; IR (KBr) ν_{max}: 3385, 2960, 2929, 2871, 1748, 1604, 1466, 1439, 1202, 1130, 1062, 995 cm⁻¹; HR-ESI-MS m/z 498.9749 ([M + H]⁺, Calcd. for C₂₀H₂₁Br₂O₅⁺, 498.9750).

Spiromastixones U (6): a white amorphous solid; UV (MeOH): λ_{max} (log ε) 230 (5.0), 282 (3.7) nm; IR (KBr) ν_{max}:

3384, 3302, 2957, 2931, 2870, 1604, 1477, 1464, 1440, 1203, 1131, 995, 938, 835 cm⁻¹; HR-ESI-MS *m/z* 339.1575 ([M + Na]⁺, Calcd. for C₁₉H₂₄O₄Na⁺, 339.1567).

Antibacterial activity assay

Compounds **1–13** were tested for the inhibitory activity against the growth of plant pathogens *X. oryzae* pv. *oryzae* (B₁), *X. oryzae* pv. *oryzicola* (B₂), *Erwinia amylovora* (B₃), *Pseudomonas syringae* pv. *lachrymans* (B₄), and *Clavibacter michiganense* subsp. *sepedonicus* (B₅). The minimum inhibitory concentration (MIC) was designated as the smallest amount of compound that limits visible microbial growth in culture.

Supplementary Materials

Supplementary material related to this article can be requested by sending E-mail to the corresponding author.

References

- [1] Xu J, Zhou L, Venturi V, et al. Phytohormone-mediated interkingdom signaling shapes the outcome of rice-*Xanthomonas oryzae* pv. *oryzae* interactions [J]. *BMC Plant Biol*, 2015, **15**: 10-25.
- [2] Nino-Liu DO, Ronald PC, Bogdanove AJ. *Xanthomonas oryzae* pathovars: model pathogens of a model crop [J]. *Mol Plant Pathol*, 2006, **7**(5): 303-324.
- [3] Mew WT. Current status and future prospects of research on bacterial blight of rice [J]. *Annu Rev Phytopathol*, 1987, **25**: 359-382.
- [4] Currie CR, Poulsen M, Mendenhall J, et al. Coevolved crypts and exocrine glands support mutualistic bacteria in fungus-growing ants [J]. *Science*, 2006, **311**(5757): 81-83.
- [5] Gonz  LM, Kaltenpoth M, Boland W. Mutualistic ants as an indirect defence against leaf pathogens [J]. *New Phytol*, 2014, **202**(2): 640-650.
- [6] Amador-Vargas S. Plant killing by mutualistic ants increases the density of host species seedlings in the dry forest of Costa Rica [J]. *Psyche-J Entomol*, 2011, **2012**: 1-6.
- [7] Heil M, Baumann B, Andary C, et al. Extraction and quantification of “condensed tannins” as a measure of plant anti-herbivore defence? Revisiting an old problem [J]. *Naturwissenschaften*, 2002, **89**(11): 519-524.
- [8] Blatrix R, Bouamer S, Morand S, et al. Ant-plant mutualisms should be viewed as symbiotic communities [J]. *Plant Signal Behav*, 2009, **4**(6): 554-556.
- [9] Arnold AE, Mejia LC, Kyll  D, et al. Fungal endophytes limit pathogen damage in a tropical tree [J]. *P Natl Acad Sci USA*, 2003, **100**(26): 15649-15654.
- [10] Han WB, Lu YH, Zhang AH, et al. Curvulamine, a new antibacterial alkaloid incorporating two undescribed units from a *Curvularia* species [J]. *Org Lett*, 2014, **16**(20): 5366-5369.
- [11] Zhang YL, Zhang J, Jiang N, et al. Immunosuppressive polyketides from mantis-associated *Dalmanella eschscholzii* [J]. *J Am Chem Soc*, 2011, **133**(15): 5931-5940.
- [12] Butler A, Carter-Franklin JN. The role of vanadium bromoperoxidase in the biosynthesis of halogenated marine natural products [J]. *Nat Prod Rep*, 2004, **21**(1): 180-188.
- [13] Niu SW, Liu D, Hu XX, et al. Spiromastixones A–O, antibacterial chlorodepsidones from a deep-sea-derived *Spiromastix* sp. fungus [J]. *J Nat Prod*, 2014, **77**(4): 1021-1030.
- [14] Niu SW, Liu D, Proksch P, et al. New polyphenols from a deep sea *Spiromastix* sp. fungus, and their antibacterial activities [J]. *Mar Drugs*, 2015, **13**(4): 2526-2540.
- [15] Sureram S, Wiyakrutta S, Ngamrojanavanich N, et al. Depsidones, aromatase inhibitors and radical scavenging agents from the marine-derived fungus *Aspergillus unguis* cri282-03 [J]. *Planta Med*, 2012, **78**(6): 582-588.
- [16] Sureram S, Kesornpun C, Mahidol C, et al. Directed biosynthesis through biohalogenation of secondary metabolites of the marine-derived fungus *Aspergillus unguis* [J]. *RSC Adv*, 2013, **3**: 1781-1788.
- [17] Lang G, Cole LA, Blunt WJ, et al. Excelsione, a depsidone from an endophytic fungus isolated from the New Zealand endemic tree *Knightia excelsa* [J]. *J Nat Prod*, 2007, **70**(2): 310-311.
- [18] Pittayakhajonwut P, Drama  A, Madla S, et al. Depsidones from the endophytic fungus bcc 8616 [J]. *J Nat Prod*, 2006, **69**(9): 1361-1363.
- [19] Kokubun T, Shiu KW, Gibbons S. Inhibitory activities of lichen-derived compounds against methicillin- and multidrug-resistant *Staphylococcus aureus* [J]. *Planta Med*, 2007, **73**(2): 176-179.
- [20] Gordana S, Igor S, Andrija S. Lichen depsidones as potential novel pharmacologically active compounds [J]. *Org Chem*, 2012, **9**: 178-184.
- [21] Motti CA, Bourne DG, Burnell JN, et al. Screening marine fungi for inhibitors of the C4 plant enzyme pyruvate phosphate dikinase: unguinol as a potential novel herbicide candidate [J]. *Appl Environ Microbiol*, 2007, **73**(6): 1921-1927.
- [22] Gupta SP, Nagappa AN. Design and development of integrase inhibitors as anti-HIV agents [J]. *Curr Med Chem*, 2003, **10**(18): 1779-1794.
- [23] Mansfield J, Genin S, Magori S, et al. Top 10 plant pathogenic bacteria in molecular plant pathology [J]. *Mol Plant Pathol*, 2012, **13**(6): 614-629.

Cite this article as: GUO Zhi-Kai, ZHU Wen-Yong, ZHAO Li-Xing, CHEN Yan-Chi, LI Sui-Jun, CHENG Ping, GE Hui-Ming, TAN Ren-Xiang, JIAO Rui-Hua. New antibacterial depsidones from an ant-derived fungus *Spiromastix* sp. MY-1 [J]. *Chin J Nat Med*, 2022, **20**(8): 627-632.